AIAA '89

AIAA 89-0158

Enhancement of Flame Blowout Limits by the Use of Swirl

Douglas Feikema, Ruey-Hung Chen, and
James F. Driscoll
Department of Aerospace Engineering
The University of Michigan, Ann Arbor, MI

27th Aerospace Sciences Meeting
January 9–12, 1989/Reno, Nevada

ENHANCEMENT OF FLAME BLOWOUT LIMITS BY THE USE OF SWIRL

A89-25741

Douglas Feikema, Ruey Hung Chen, James F. Driscoll
Department of Aerospace Engineering
The University of Michigan, Ann Arbor, MI 48109-2140

Abstract

The blowout limits of a number of swirl stabilized flames were measured and the trends are explained by applying the concepts proposed in recent flame blowout theories, which previously have been applied only to non-swirling flames. It is shown that swirl flame blowout limits can be compared to well-known limits for non-swirling simple diffusion flames by using the proper nondimensional parameter, i.e., the inverse Damkohler number $(U_F/d_F)/(S_L^2/\alpha)$. Unlike most previous work, four parameters were systematically varied: the fuel tube diameter (d_F), the fuel type and thus reaction rate, which is related to the maximum laminar burning velocity (S_L), the coaxial air velocity (U_A), and the swirl number.

Results show that the maximum fuel velocity (U_F) and thus the maximum heat release rate for a swirl flame is as much as four times larger than that for a non-swirling flame. Blowout velocity (U_F) increases with burner size (d_F) and laminar burning velocity squared (S_L^2); this is similar to non-swirling flames except that a new parameter that includes swirl number must be added. The major reason why swirl increases the stability of a flame is because of a flame-vortex interaction. The toroidal recirculation vortex reduces the centerline velocity below that of a non-swirling flame and the analysis shows that this is strongly stabilizing.

1. Introduction

The purpose of this paper is to report some systematic measurements of the blowout limits of swirl-stabilized flames and to explain the measured trends using concepts that have been proposed in recent theory (1-3). The theory has been successfully used in non-swirling flames but has not been applied to swirl flames. The trends reported herein can be used to assist future efforts to develop a general blowout theory for swirling flames. The swirl flame that was studied can be described, in simplest terms, to be a fuel jet that passes through the center of a strong toroidal vortex. The vortex is the recirculation zone that is created when swirl is added to a coaxial airstream that surrounds the fuel jet (4-5). The resulting flame-vortex interaction that occurs is known to stabilize the flame, but the reasons for the stabilizing effects are still in dispute. (The term stabilizing factors in the present work denotes factors that prevent blowout). Properties of stable swirl flames have been well documented (4-9) because such flames are commonly used in gas turbine engines, industrial burners, and in advanced ramjet designs (10).

Some of the major questions that the present work addresses are as follows:

(a) Which of several proposed mechanisms correctly explains how the flame-vortex interaction (which is caused by the swirl) increases the stability of a flame?
(b) How do blowout limits of swirl flames scale as the burner size is increased and the fuel type is varied?
(c) What parameter should one use to compare blowout limits of swirl flames to the limits for a simple jet flame in order to see if swirl is indeed beneficial?

In some cases, a swirl flame is less stable than a simple jet flame. The goal of the present work is to systematically vary the burner size, fuel type, swirl number and coaxial air flowrate in order to provide some data that will help to answer the above questions.

Some reasons why swirl enhances flame stability have been offered by Leuckel and Fricker (11), Rawe and Kremer (12) and Yuasa (13). In addition, the blowout limits of some swirl flames (for a limited range of conditions) also have been reported by Tangirala, et al. (6), Whitelaw (14), and others (15,16). It is clear from the above work that there are three ways in which flame blowout occurs, which can be labeled: (a) the excessive fuel velocity limit (or the "rich limit"), (b) the excessive swirl and/or air velocity limit (or the "lean limit") and (c) the minimum swirl limit, which leads to the disappearance of the recirculation vortex.

The effect of swirl on flame blowout still is in dispute. At present, there are four different mechanisms that attempt to explain the effect of swirl.

(1) Swirl is believed to be a stabilizing factor because it increases the turbulent burning velocity of the base of a lifted flame (11,12,16). The base region of a lifted, initially non-premixed flame most likely is partially premixed. Swirl should increase the turbulent burning velocity at the flame base because it increases the local velocity fluctuations by a factor of three (6) and because the recirculation vortex should create larger regions of locally premixed fuel and air than are found in non-swirling flames.
(2) A different proposal is that the recirculation vortex acts as a heat source, forcing hot products to move upstream and mix with the partially premixed reactants (5). Thus swirl can increase the residence time during which fuel, air and hot products can coexist, which could be an important stabilizing factor near the blowout limit. Using this argument, it also has been postulated that excessive swirl should be a destabilizing factor when the recirculation vortex becomes so large that it entrains too much cold outside air (13). For such conditions

there would be cool gas, rather than hot gas, that is forced upstream to mix with the partially premixed reactants.

(3) A third reason that could explain why swirl is a stabilizing factor is that swirl can create stagnation points that act as bluff-body flame holders. Either the stagnation point at the upstream end or at the downstream end of a recirculation vortex could be a point of flame attachment.

(4) Another effect of swirl is that it can greatly increase the rate of strain imposed on a flame. The recirculation zone is, in fact, a large vortex that has greater circulation strength than the eddies associated with simple jets.

2. Previous Analysis of Blowout Limits for Non-Swirling Flames

In order to explain the measurements that are reported herein, it is necessary to cite two analyses that explain the blowout of non-swirling jet flames. The first approach was postulated by Vanquickenbourne and Van Tiggelen (17) and was extended by Kalghatgi (18,19). A flame is assumed to blow out when the local gas velocity near centerline (U_{CL}) exceeds the local burning velocity (S_T) of the flame base, which is assumed to be partially premixed. This simple concept is difficult to implement because the degree of local premixing is not known, the relation between the burning velocity and turbulence level in any premixed flame is in dispute, and it is a serious error to use mean concentration levels to infer the instantaneous concentration. That is, at a given location one may find very fuel-rich conditions at some times and fuel-lean conditions at other times such that the mean equivalence ratio is stoichiometric; a model could predict that such a location is ideal for flame stabilization when in fact no flame could exist there.

Kalghatgi's analysis employed an empirical relation for burning velocity S_T (20) such that at the flame liftoff position z:

$$U_{CL}(z) = S_T(z) = S_L \sqrt{\frac{u' \ell}{\alpha}} \qquad (1)$$

where S_L is the maximum laminar flame speed and α is the thermal diffusivity. The quantity ℓ is the mixing length in the jet; it is proportional to the liftoff height z. Kalghatgi then uses his own empirical observation that blowout occurs when the liftoff height z is 0.75 times the length of the attached flame, which is known to be proportional to the fuel tube diameter d_F (21). Velocity fluctuations u' are assumed to be proportional to U_{CL}, and U_{CL} can be shown to be $U_F\, d_F/z$ since the jet is self-similar and the momentum flux, which is the integral of $\rho\, U^2(z)\, 2\pi r dr$, is conserved. U_F is the fuel exit velocity. Simple substitution of these quantities into Eq. 1 yields a nondimensional relation for blowout velocity U_F:

$$\frac{U_F/d_F}{S_L^2/\alpha} = 0.017 \left(\frac{\alpha}{\nu}\right) \left(\frac{\rho_a}{\rho_F}\right)^{1.5} \left(4 \frac{\theta_E}{\theta_S} \left(\frac{\rho_F}{\rho_a}\right)^{0.5} - 5.8\right) \qquad (2)$$

The right hand side of Eq. 2 depends on the fuel properties ρ_F, thermal diffusivity α and kinematic viscosity ν. The quantities θ_E and θ_S are fuel mass fractions at the jet exit and in a stoichiometric mixture, respectively. Kalghatgi shows that Eq. 2 is in good agreement with his measurements of U_F. Thus, for simple jet flames, the blowout velocity U_F is proportional to d_F and S_L^2.

A different approach was suggested by Broadwell, Dahm and Mungal (1); this analysis will be referred to as the BDM approach. Blowout is assumed to occur when the local fluid mechanical mixing time, which is $U_{CL}(z)/\delta(z)$, exceeds the chemical reaction rate, which is proportional to S_L^2/α. Such a concept is analogous to the criterion that was successfully used by Marble and Zukowski to explain the blowout of premixed flames stabilized by a rod (22). $U_{CL}(z)$ is the centerline axial velocity which varies as $U_F\, d_F/z$ and δ is the jet halfwidth that is proportional to z. The liftoff position (z) at blowout in the BDM analysis is assumed to be proportional to the length of the attached flame, which is explained to be the distance required to mix fuel and air to their stoichiometric proportions. Thus z is proportional to the fuel tube diameter d_F. The BDM criterion that blowout occurs at a universal value of the ratio of the local mixing time to chemical reaction time leads to a blowout velocity U_F given by:

$$\frac{U_F/d_F}{S_L^2/\alpha} = 0.21\, \Psi 2 \left(\frac{\rho_F}{\rho_A}\right)^{1/2} \qquad (3)$$

where Ψ is the stoichiometric air-to-fuel mass ratio. Thus the final result of the BDM analysis is similar to that of Kalghatgi (Eq. 2). Both Eqs. 2 and 3 agree well with experiments even though the right hand sides are functionally different.

The major advantage of the BDM approach is that it recently has been successfully applied to two geometries that are more complicated than a simple jet flame. Dahm and Mayman (2) and Dahm and Dibble (3) have extended the BDM concepts to correctly predict blowout curves for the case of a simple jet surrounded by a coaxial air flow having a finite diameter, as well as for the somewhat different case of coflowing air of infinite extent. In both cases the airflow dramatically changes the blowout limits; air velocity as low as 2% of the fuel velocity can cause blowout, and a new limit appears which is a minimum fuel velocity. The fact that Dahm's analysis can correctly predict these new physical trends as well as predict both the shape and magnitude of the blowout curves, using no new empirical constants, is very encouraging.

3. Experimental Apparatus

A schematic of the swirl-stabilized flame apparatus is shown in Fig. 1. The swirl generator consists of four tangential air inlets that mix tangential air with axial air upstream of the burner. The swirling coaxial airflow surrounds a central fuel tube that injects fuel in the axial direction. Three different sized burners were used, whose dimensions are given in Table 1. In all cases, the ratio of the fuel tube inner diameter (ID) to the air tube ID was constant; the ratio of the fuel tube ID to the fuel tube outer diameter (OD) also was constant. Air tube throat diameter is denoted d_A and was as large as 3.14 cm; fuel tube ID is denoted d_F and was as large as 0.48 cm. Three different fuels were used: methane, 0.67 methane with a 0.33 hydrogen by volume, and 0.45 methane with 0.55 hydrogen, as listed in Table 1. Flowrates were metered using a system of 15 calibrated choked orifices and 4 rotameters to cover a wide range of conditions. A small correction to fuel velocity was made for compressibility effects for about 10% of the data collected. To obtain a strong recirculation vortex, a diverging metal quarl section is placed downstream of the cylindrical throat; the quarl wall is inclined at 30 degrees with respect to the axis. Additional experimental details are given in Ref. 6.

The swirl number S in this study is identical to the conventional definition given by Chigier (4), i.e., S is the ratio of the flux of angular momentum passing through the throat to the flux of axial momentum, divided by the throat radius R. Thus:

$$S = \int (\rho\, U_\theta^2\, 2\pi r dr \,/\, \int \rho (U_z - U_\theta/2)\, 2\pi r dr \cdot R \qquad (4)$$

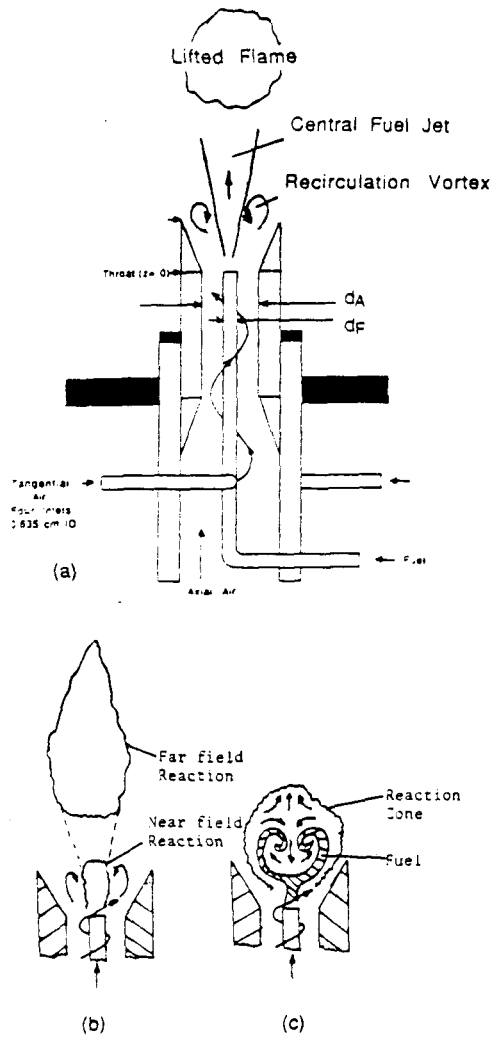

Figure 1. Schematic of Three Types of Swirl-Stabilized Flames: (a) Lifted flame with penetrated fuel jet; (b) Type 1: Long jet-like flame at blowout. Reaction in far and near fields; (c) Type 2: Short, strongly recirculating flame at blowout.

Use of Eq. 4 eliminates any need to measure static pressure (23). Laser velocimetry was used to measure profiles of u_θ and U_z within the Vycor glass throat and thus the swirl number S was deduced using Eq. 4. It was found that a convenient way to monitor S was to monitor the mass flow rates of the axial air (m_A) and tangential air (m_θ) to first determine a geometric swirl number (S_g) which is defined as (24):

$$S_g = \frac{\pi r_o R}{A_t}\left(\frac{m_\theta}{m_\theta + m_A}\right)^2 \qquad (5)$$

A_t is the total area of the four tangential air inlets and r_o is the radial location of the inlets. Both S and S_g were measured for 17 different conditions and in all cases S was found to be 0.25 S_g to within a standard deviation of ± 6% (9). Using this calibration, it was possible to deduce S directly from the mass flow measurements.

4. Types of Flames Observed

Just prior to flame blowout, three distinct types of flames were observed, as shown in Fig. 1. These three types of flames are denoted: (a) lifted flames, which look like lifted simple jet flames; (b) type 1 jet-like flames, which look like long, attached jet flames but blow out suddenly without lifting off; and (c) short, Type 2 flames which also blow out suddenly without rising (i.e., without appreciable liftoff).

The lifted flame (Fig. 1a) is blue near the base, although the downstream region may be yellow. The blue base region may indicate that appreciable fuel-air mixing occurs in the liftoff region. The liftoff height of these swirl flames differs from that of a simple jet flame. For the swirl flames, the liftoff height is constant and independent of fuel velocity; the flame appears to stabilize in the wake of the recirculation zone. For a simple jet flame, liftoff height varies; it increases with fuel jet velocity. The second type of blowout occurs for Type 1 jet-like flames (Fig. 1b). These long flames blow out without appreciable liftoff, indicating that the upstream portion of the recirculation zone is stabilizing the flame. When the fuel velocity exceeds a critical value, apparently the conditions in the downstream region of the recirculation zone are not favorable for flame stabilization so the entire jet flame suddenly blows out. The third type of flame is the short, Type 2 flame which always appears to be blue. This type of flame has a strong recirculation zone and blowout occurs when the fuel velocity is reduced significantly. The short Type 2 flames do not blow out due to excessive fuel velocity, but because the lean flame is strained out by the strong vortex (i.e., recirculation zone).

5. Results: Effects of Swirl, Coaxial Air

The blowout limits for the intermediate size burner and methane fuel are shown in Fig. 2. The first observation is that the blowout limits are defined by a peninsula-shaped curve. Two questions arise that are discussed below: how does existing theory explain the observed shape of the curves and why does the size of the peninsula-shaped stable region increase as swirl is increased? It is first noted that all of the blowout curves in Fig. 2 intercept the y axis at U_F = 61.7 m/sec; this point corresponds to the case of a simple jet flame with no coaxial air. This y-axis is intercept in Fig. 2, as well as the corresponding y-axis intercepts measured for the different burner sizes, all agree to within 10% with the results of Kalghatgi's findings for non-swirling jet flames [Eq. 2].

The fact that the stable region in Fig. 2 is peninsula-shaped indicates that blowout can be caused by either increasing fuel velocity above a "rich limit" or by reducing U_F below a "lean limit." The ratio of these two limits is the turndown ratio, which should be maximized for practical combustors. Figure 2 shows that the turndown ratio can be increased by increasing the swirl. It is expected that the lean limit in Fig. 2 should pass through the origin; if it intercepted the x-axis, infinitely lean flames would be possible. It is noted that each curve in Fig. 2 extends to the right to only a certain extent; there is a maximum air velocity U_A above which no stable flame is possible. This implies that for a given air velocity, there is a minimum swirl number limit. For example, for U_A = 28 m/sec in Fig. 2, the minimum swirl number is 0.25. Operation at S below 0.25 produces a peninsula-shaped region that does not extend sufficiently far to the right in Fig. 2 to overlap the vertical line U_A = 28 m/sec.

One of the curves in Fig. 2, namely the zero swirl curve, can be predicted accurately by the existing theory of Dahm and Mayman (2). Dahm, and to a limited extent Vranos [25] and Yuasa (13), also have measured zero-swirl blowout curves similar to the one in Fig. 2.

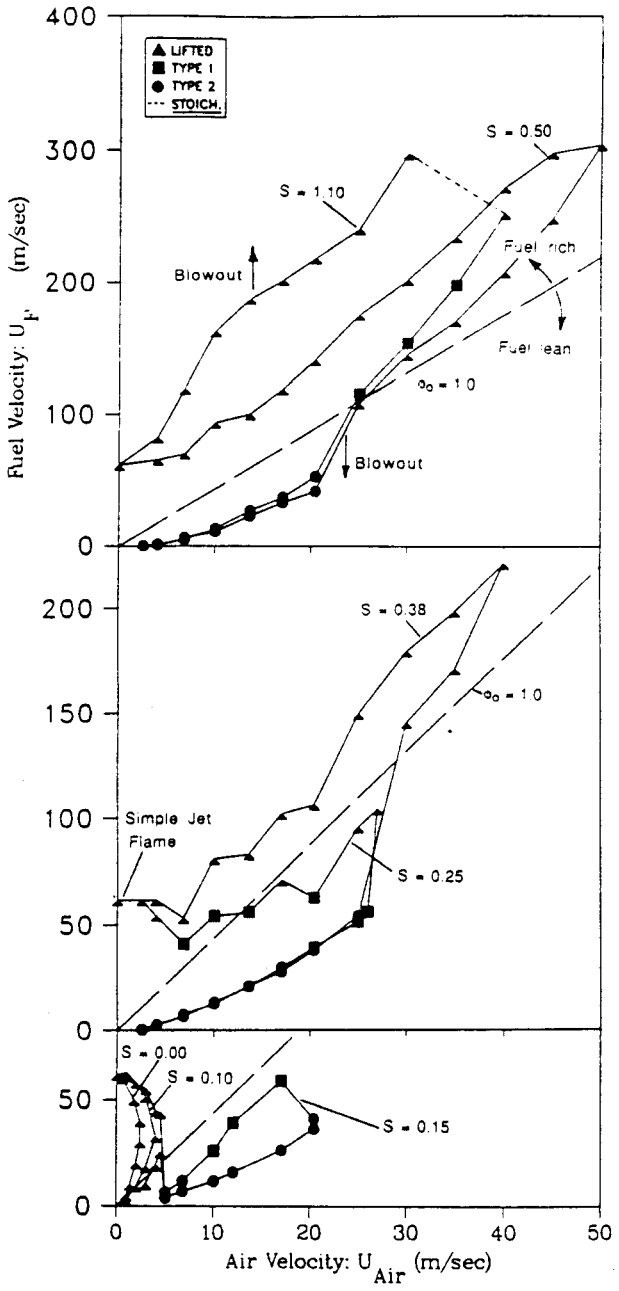

Figure 2. Maximum and Minimum Fuel Blowout Velocities for the Intermediate Sized Burner and Methane Fuel. (d_A = 0.22 cm, d_F = 0.34 cm; flame shape at blowout: ▲ = lifted, ■ = long, jet-like, no liftoff, ● short, recirculating, no liftoff.

It is concluded from the zero swirl curve of Fig. 2 that coaxial air alone (with no swirl) has a destabilizing effect on a flame. That is, the maximum fuel velocity in Fig. 2 is reduced from 61.7 m/sec for zero coaxial air, to 40 m/sec for air velocity of 2.4 m/sec. For air velocity above 2 m/sec, the flame is not stable for any fuel velocity. It also can be concluded from Fig. 2 that even small amounts of swirl have a stabilizing effect; the semicircular stable region for S = 0.1 is larger than the stable region for zero swirl. However, the low swirl, non-recirculating flames are still less stable than the pure diffusion flame (i.e., the y axis intercept in Fig. 2) because the stabilizing effects of swirl do not yet exceed the destabilizing effects of coaxial air. That is, the recirculation zone is not of sufficient strength to dramatically enhance the mixing of fuel and air.

On the other hand, a sufficient amount of swirl has a strong stabilizing effect on the flame. Figure 2 quantifies this effect in an unambiguous manner. It is seen that the fuel velocity can be increased by a factor of five over that of a simple jet flame (i.e. from 61.7 m/sec to 298 m/sec). This is a significant improvement and allows the burner to provide five times the heating power (in kilowatts) of a non-swirling flame having the same fuel tube diameter. Although the stabilizing effects of swirl are well known, quantitative comparisons of swirl burners to non-swirling jet flames, such as Fig. 2, are few. Yuasa (13) reports a fourfold improvement in the maximum fuel velocity due to swirl.

Figure 3 shows another way to plot the flame blowout limits that can be more useful for practical design. In practical cases the overall fuel equivalence ratio may be specified. Figure 3 shows that there is a swirl number that is optimum for a given equivalence ratio. For overall rich conditions at the burner exit (i.e., when outside entrained air is available) such as $1/\Phi = 0.5$, it is seen that the most stable flame is the one with the highest swirl number of 1.1. For fuel lean conditions such as $1/\Phi = 2.0$, lower swirl is seen to be somewhat preferable. Thus rich flames are more stable if high swirl is provided while lean flames are limited to smaller amounts of swirl, which is in agreement with observations of Leuckel (11). It is believed that rich flames benefit from the increased mixing of air into the flame caused by swirl-induced vortex, while lean flames extinguish when all the available air is rapidly mixed with the fuel.

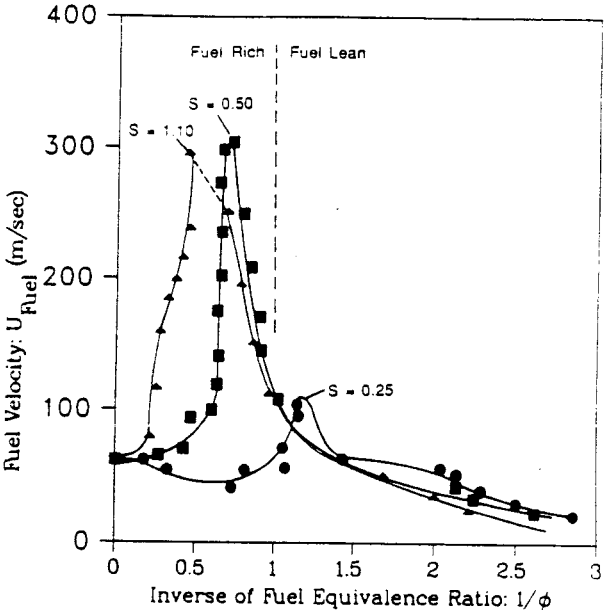

Figure 3. Optimum Swirl Number for Rich and Lean Conditions.

6. Effect of Burner Size, Fuel Type

The effect of burner size on flame blowout can be observed by comparing Figs. 2, 4 and 5. Three geometrically similar burners were operated using methane fuel tube diameters were 0.22 cm, 0.34 cm and 0.48 cm as given in Table 1. For zero coaxial air, the blowout velocities of the simple jet flames are observed to increase from 39.4 m/sec (Fig. 4) to 61.7 m/sec (Fig. 2) to 80.5 m/sec (Fig. 5) as fuel tube diameter increases. Thus, the absolute values of U_F at blowout for no swirl or coaxial air are

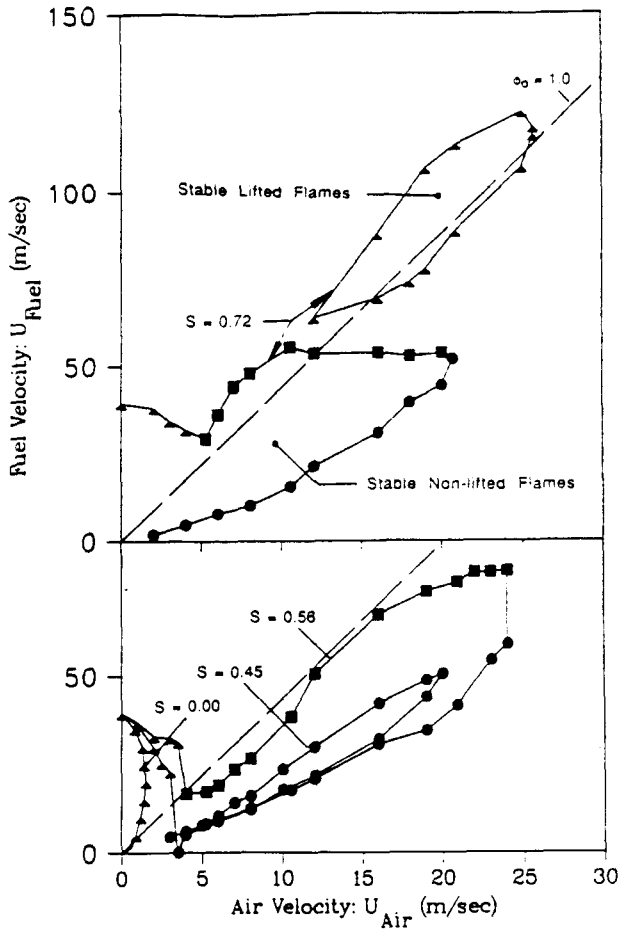

Figure 4. Maximum and Minimum Fuel Blowout Velocities for the Smallest Burner and Methane Fuel. (d_A = 1.44 cm, d_F = 0.22 cm; flame shape at blowout: ▲ = lifted, ■ = long, jet-like, ●, short, recirculating)

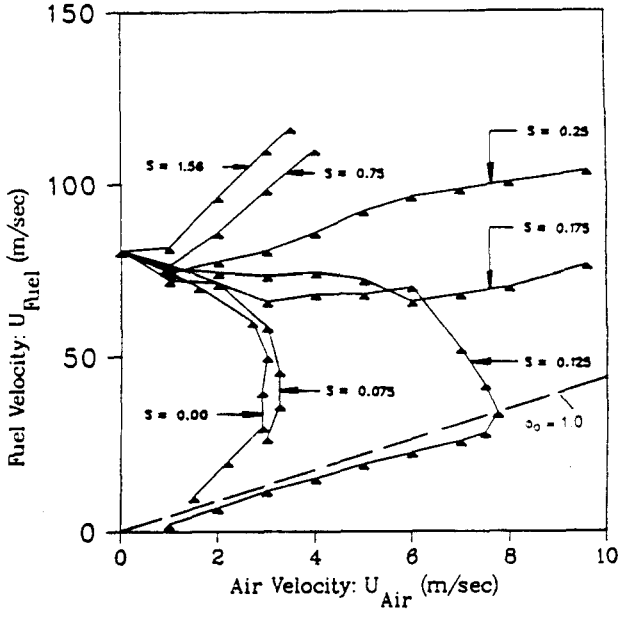

Figure 5. Fuel Velocity at Blowout for Largest Burner and Methane Fuel. (d_A = 3.14 cm, d_F (inner) = 0.48; symbols same as Figure 4.)

in good agreement with Kalghatgi's previous data, as represented by Eq. 2, as well as with the BDM analysis, as represented by Eq. 3. As coaxial air and swirl is added, the general shapes of the curves in Figs. 4 and 5 are similar to those in Fig. 2. It is noted that for the conditions of Fig. 4, i.e., using the smallest burner, the stable region is no longer peninsula-shaped but a disjoined stable region occurs. These lifted flames only can be created by first increasing the velocity of the fuel jet such that it penetrates the recirculation zone, and then igniting the flame. Unlike a jet flame, these particular lifted flames cannot be achieved by starting with an attached flame and then increasing fuel velocity.

The effect of adding hydrogen to the methane fuel is shown by comparing Figs. 6 and 7 to Fig. 4. The burner size is the same for Figs. 4, 6 and 7 but the amount of hydrogen in the fuel is 0%, 33% and 55% by volume, respectively. In all cases, the methane-hydrogen mixture was premixed in a high pressure tank and all measurements were made with the same tank of fuel to insure repeatability of fuel composition. The blowout velocity for zero swirl and zero coaxial air increases from 39.4 m/sec (Fig. 4) to 90.2 m/sec (Fig. 6) to 182.8 m/sec (Fig. 7) as hydrogen is added. These blowout velocities for non-swirling H_2-methane jet flames do not agree with Kalghatgi's correlation (Eq. 2) which he showed to be valid for pure methane, pure hydrogen, and methane-inert fuel mixtures. Results of the present study for pure methane with no coaxial air do agree with Kalghatgi's Eq. 2 for these burner sizes. The reason why the hydrogen-methane mixture yields a blowout velocity that is larger than that which is predicted by Eq. 2 is probably due to the uncertainty in the laminar burning velocity of CH_4-H_2 mixtures, which is required to use Eq. 2. To use Eq. 2, the maximum laminar burning velocity (S_L) of the two H_2-CH_4 mixtures were measured using a laminar premixed conical flame; results agreed with Ref. 26. Thermal diffusivity and other properties of the mixture were determined using Ref. 27.

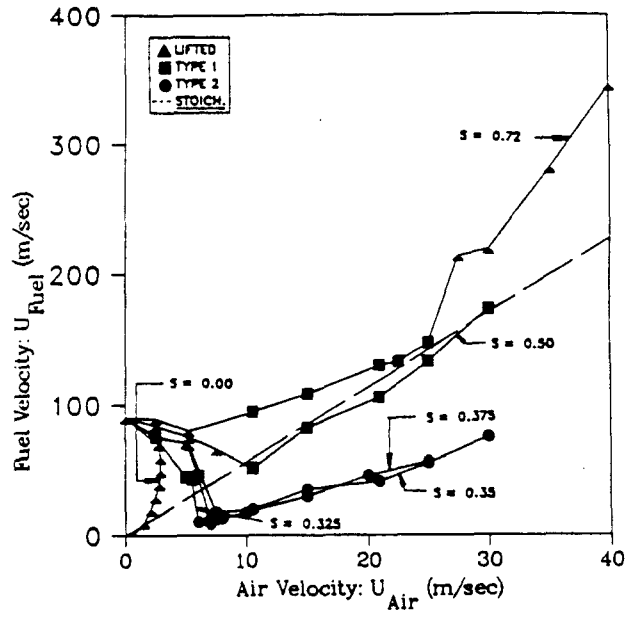

Figure 6. Effects of 33% Hydrogen Enrichment of Methane Fuel on Blowout Limits of Smallest Burner. (d_A = 1.44 cm, d_F (inner) = 0.22 cm, symbols same as Figure 4.)

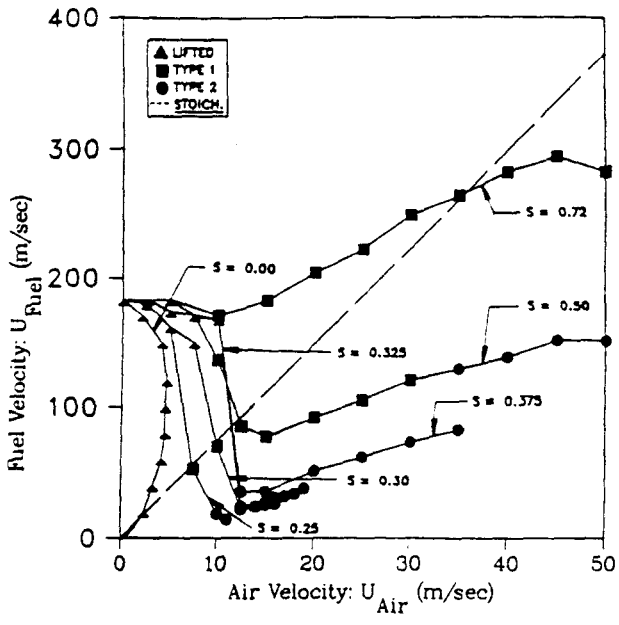

Figure 7. Effect of 55% Hydrogen Enrichment of Methane Fuel on Blowout Limits of Smallest Burner (symbols same as Figure 4.)

7. Analysis and Correlation of Limits

Previous analyses of non-swirling flames (1,2) have shown that blowout can be explained as the condition that occurs when a local inverse Damkohler number $(U_{CL}/\delta)/(S_L^2/\alpha)$ exceeds some critical value which leads to Eq. 3. Since U_{CL} and δ are local conditions at the location where the lifted flame blows out, it is necessary to relate u and d to the operating parameters U_F, d_F, S, etc.

It is proposed that U_{CL} and δ can be properly related to swirl flame parameters in the following way. One can represent a lifted swirl flame as a fuel jet that has penetrated through a toroidal vortex, as shown in Fig. 1. The effect of swirl therefore is to reduce the local centerline velocity U_{CL}, at every axial location, below that of the non-swirling case (U_j), and this should have a stabilizing effect on a flame. Thus:

$$U_{CL}(z) = U_j(z) - U_v(z) \qquad (6)$$

where subscript j denotes conditions within a non-swirling jet, and U_v is some velocity induced by the recirculation vortex at some downstream location where the lifted flame blows out. While the exact form of U_v is not known, the experimental data show that U_v for a Type 1 penetrated type of swirl flame scales as (6):

$$U_v \sim U_A \cdot S \qquad (7)$$

The proper scaling for U_j is $U_j \sim U_F\, d_F/z$, since the total momentum flux for a jet is conserved. The characteristic mixing distance δ is expected to scale with burner size, i.e., d_F, on a manner similar to non-swirling jet flames. Therefore setting $(U_{CL}/\delta)\,/\,(S_L^2/\alpha)$ equal to the right hand side of Eq. 3 and using Eqs. 6 and 7, it follows that:

$$\frac{U_F/d_F}{S_L^2/\alpha} = c_3 + \left(\frac{U_A/d_F}{S_L^2/\alpha}\right) S \cdot c_4 \qquad (8)$$

where c_3 depends on Ψ, ρ_F and ρ_A. Equation 8 indicates that the maximum fuel velocity U_F should scale linearly with U_A and the slope of the U_F vs. U_A line should be proportional to swirl number S.

To test the scaling ideas that lead to Eq. 8, the data in Figs. 2 and 4 were replotted in Figs. 8 and 9; only the maximum fuel velocity blowout limits are shown. It is seen from the curves in Figs. 8 and 9 that U_F does scale linearly with U_A and that the slope of the U_F vs. U_A curve is proportional to swirl number. Thus the trends in Figs. 8 and 9 are in agreement with those predicted by Eq. 8. The curves in Figs. 8 and 9 are replotted as Figs. 10 and 11 using the parameters suggested by Eq. 8. It is seen that the various blowout curves collapse to a single curve in Fig. 10 and in Fig. 11.

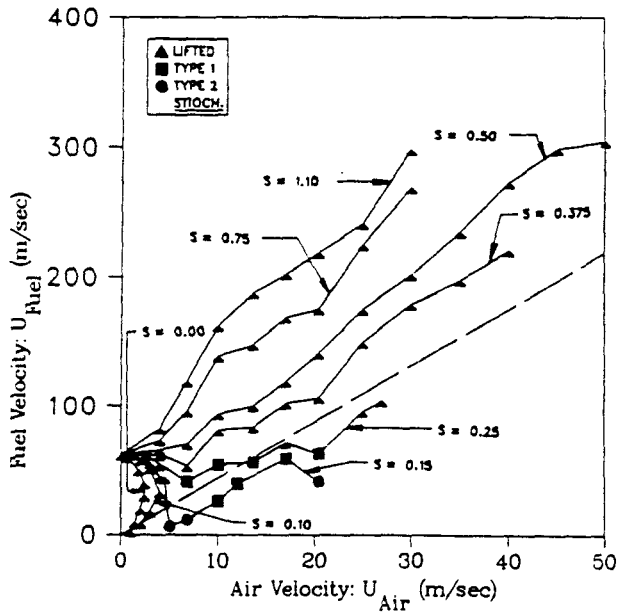

Figure 8. Maximum Fuel Velocity Limit for Intermediate Size Burner Using Methane.

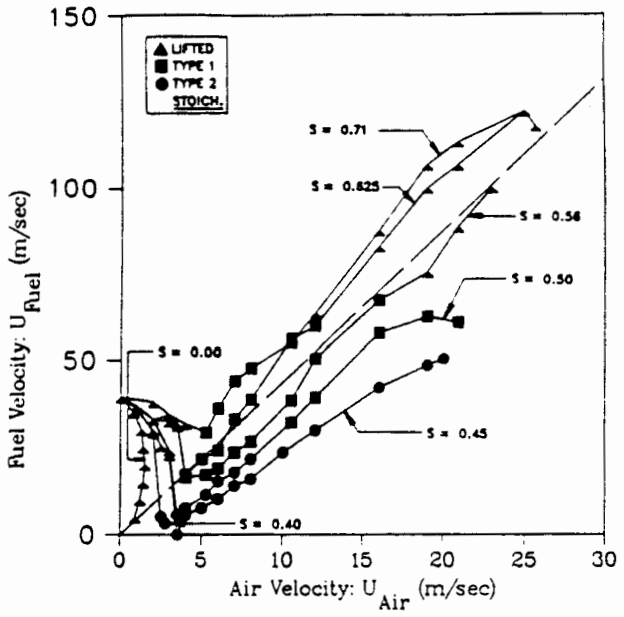

Figure 9. Maximum Fuel Velocity at Blowout for Smallest Swirl Burner Using Methane.

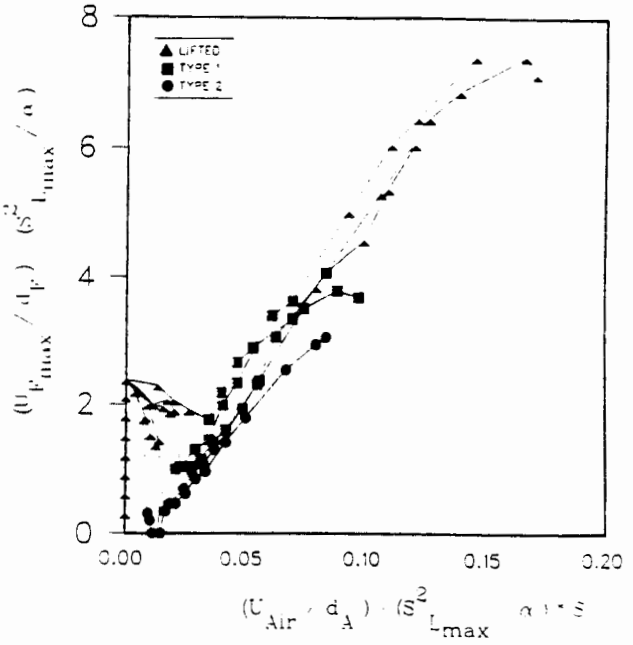

Figure 11. Collapse of Numerous Blowout Curves in Figure 9 to a Single Curve By Plotting Parameters Suggested by Eq. 9. Smallest Burner.

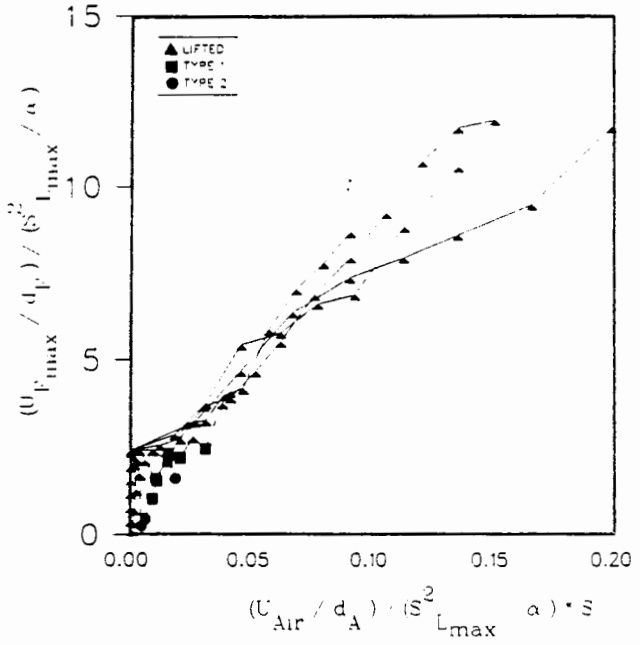

Figure 10. Collapse of Numerous Blowout Curves in Figure 8 to a Single Curve By Plotting Parameters Suggested by Eq. 8. Intermediate Sized Burner.

Another parameter that was varied in the diameter ratio (d_F/d_A) of the fuel tube to the air tube. Figure 12 shows that in all cases the blowout curves remain peninsula-shaped, with maximum fuel velocity occurring for rich flames. Somewhat better flame stability (i.e., larger values of U_F/d_F) occurs for the smaller diameter ratio.

8. Acknowledgement

The research reported herein is supported by the Gas Research Institute under contract 5087-260-1443. The contract monitor is J. Kezerle.

9. References

1. Broadwell, J. E., Dahm, W.J.A., and Mungal, M. G., 20th Symp. on Combustion, p. 303, 1985.

2. Dahm, W.J.A. and Mayman, A. G., Univ. of Michigan Report GRI 5087-260-1443-2; submitted for publication, 1988.

3. Dahm, W.J.A. and Dibble, R. W., 22nd Symp. on Combustion, 1988.

4. Beer, J. M. and Chigier, N., Combustion Aerodynamics, Applied Science Publishers, London, 1972.

5. Syred, N. and Beer, J. M., Comb. Flame 23, 143, 1974.

6. Tangirala, V. and Driscoll, J. F., Comb. Sci. Tech., 60, 1-3 p. 143, 1988.

7. Tangirala, V., Chen, R. H. and Driscoll, J. F., Comb. Sci. Tech. 51, p. 75, 1987.

8. Chen, R. H. and Driscoll, J. F., 22nd Symp. on Combustion, 1988.

9. Chen, R. H., Driscoll, J. F., Kelly, J., and Namazian, M., to appear.

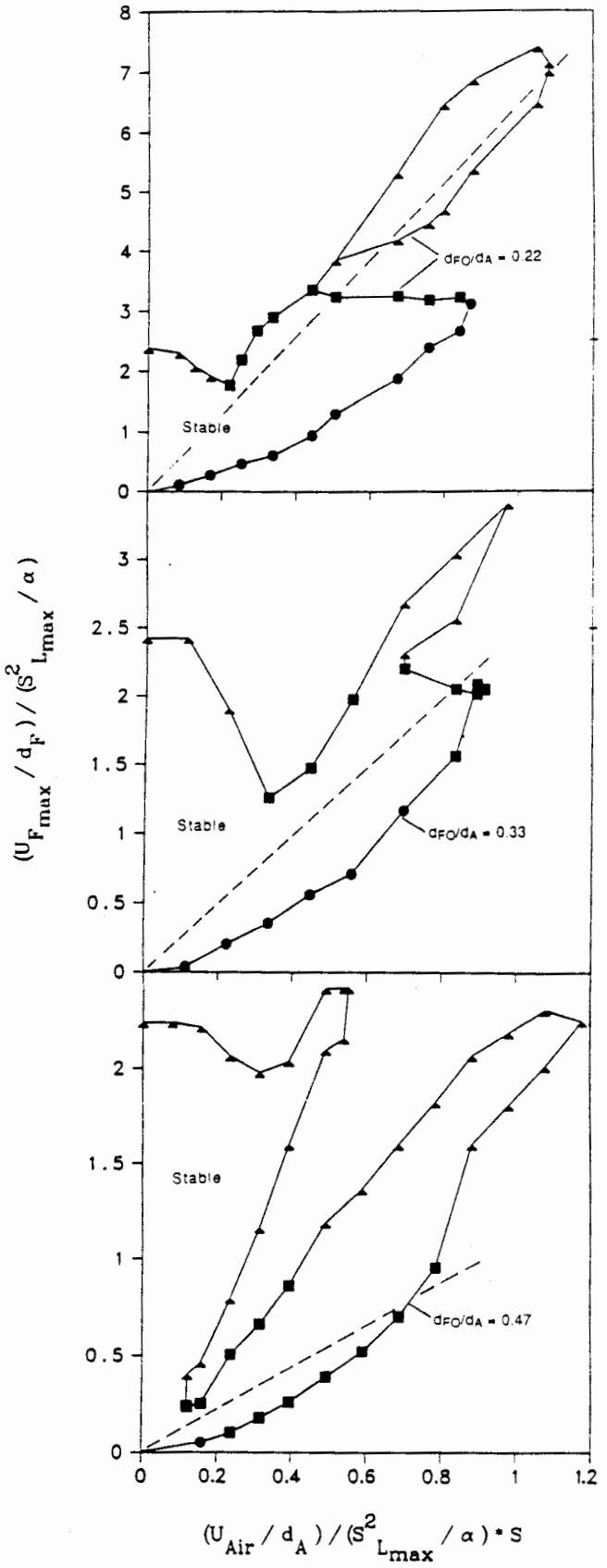

Figure 12. Effect of Diameter Ratio d_{FO}/d_A on Flame Blowout Limits, S = 0.72.

Table 1. Parameters Describing the Three Geometries and Three Fuels Used for the Swirl-Stabilized Flames

System Configuration	A	B	C	D	E
Fuel	CH_4	CH_4	CH_4	0.67 CH_4 & 0.33 H_2 by volume	0.45 CH_4 & 0.55 H_2 by volume
d_A (cm)	3.14	2.22	1.44	1.44	1.44
d_F (inner)(cm)	0.48	0.34	0.22	0.22	0.22
d_A/d_F (inner)	6.5	6.5	6.5	6.5	6.5
d_F (outer)/d_F(inner)	1.42	1.41	1.44	1.44	1.44
S (max)	1.55	1.10	0.72	0.72	0.72
Re (max) $= U_A d_A/\nu$	20,000	52,000	25,000	48,000	48,000
Q_{max} (K watts) Heat Release	70.0	75.5	15.5	33.4	62.0

10. Buckley, P. L., Craig, R. R., Davis, D. L. and Schwartzkopf, K. G., AIAA J. 21, 733-740, 1983.
11. Leuckel, W. and Fricker, N., J. Inst. Fuel 49, 152, September 1976.
12. Rawe, R. and Kremer, H., 18th Symp. on Combustion, p. 667, 1981.
13. Yuasa, S., Comb. and Flame 66, p. 181, 1986.
14. Milosavljevic, V., Taylor, A.M.K.P., and Whitelaw, J. H., Comb. Flame, to appear.
15. Godoy, F. and Lockwood, F. C., Comb. Sci. Tech. 44, 319, 1987.
16. Hillemanns, R., Lenze, B., and Leuckel, W., 21st Symp. on Combustion, p. 1445, 1986.
17. Vanquickenbourne, L. and Van Tiggelen, A., Comb. Flame 10, 59, 1966.
18. Kalghatgi, G., Comb. Sci. Tech. 26, p. 233, 1981.
19. Kalghatgi, G., Comb. Sci. Tech. 41, p. 17, 1984.
20. Andrews, G. E., Bradley, D. and Lwakabamba, S. B., Comb. and Flame, 24, 285-304, 1975.
21. Hawthorne, W. R., Weddell, D. S. and Hottel, H. C., Third Symposium (International) on Combustion, 31, 1943.
22. Lewis, B. and Von Elbe, G., Combustion Flames and Explosions of Gases, Academic Press, 1961.
23. Ribiero, M. M. and Whitelaw, J. H., J. Fluid Mech. 96, 769, 1980.
24. Claypole, T. C. and Syred, N., 18th Symp. on Combustion, p. 1489, 1981.
25. Vranos, A., Taback, E. D., and Shipman, C. W., Comb. and Flame 12, p. 253-260, 1968.
26. Strehlow, R., Combustion Fundamentals, Fig. 8.6a, McGraw-Hill Book Co., New York, 1984.
27. Technical Data Book - Petroleum Refining, American Petroleum Institute, 3rd Ed., 1976.